3-D Seismic Evidence of the Effects of Carbonate Karst Collapse on Overlying Clastic Stratigraphy and Reservoir Compartmentalization

B. A. Hardage (hardageb@begv.beg.utexas.edu; 512-471-0300)
Bureau of Economic Geology
The University of Texas at Austin
University Station, Box X
Austin, TX 78713-8924

D. L. Carr
D. E. Lancaster
J. L. Simmons, Jr.
R. Y. Elphick
V. M. Pendleton
R. A. Johns

Introduction

The results described here represent part of the work done during one phase of the Secondary Gas Recovery (SGR) project, a research and field demonstration program sponsored by the U.S. Department of Energy, the Gas Research Institute, and industry partners. The basic philosophy of this program is to combine off-the-shelf technologies with modern research concepts to demonstrate how to develop improved models of heterogeneous gas reservoirs. A specific objective of these SGR studies has been to determine how various depositional processes affect reservoir compartmentalization; thus, field study sites have been selected so that the effects that specific depositional systems have on the internal architecture and complexity of gas reservoirs can be studied.

One previously reported SGR study focused on fluvial gas reservoir facies deposited in a *high-accommodation* basin setting (Hardage et al., 1994), where the term *accommodation space* is defined as that volume below the deepest erosional surface within a depositional basin that is available for accumulation of sediment. In contrast, the study site described in this paper was selected because we wished to analyze how gas reservoirs are compartmentalized by a fluvio-deltaic system depositing sediment in a *low- to moderate-accommodation* basin setting. The search for an appropriate study site led us to Boonsville field in the Fort Worth Basin (Fig. 1).

At Boonsville field, gas production occurs throughout the Bend Conglomerate interval, a Middle Pennsylvanian clastic section having a thickness of 900 to 1,300 ft (275 to 400 m) in our study area, with the base of the interval being a little less than 6,000 ft (1,830 m) deep. Previous studies have established that the Bend Conglomerate section was deposited in a fluvio-deltaic environment (Thompson, 1982). These productive Bend Conglomerate clastics are underlain by extensive Paleozoic carbonates, the deepest carbonate section being the Ellenburger Group of Ordovician age.

We selected a 26-mi^2 (67-km^2) area encompassing approximately 200 wells (Fig. 2) where we recorded 3-D seismic data and built an extensive geologic, petrophysical, and engineering data base to study reservoir heterogeneity and compartmentalization within the Bend Conglomerate interval. We began this study with the thought that the only deep-origin geologic phenomenon that might affect reservoir compartmentalization in the shallower Bend Conglomerate clastics would perhaps be basement faults. However, our interpretation of the 3-D seismic data revealed that numerous *karsts* (that is, severe, unconformity-related solution weathering of limestone) occurred in the deep Ellenburger (Ordovician) carbonates and that karst-generated collapse created breccia pipes and structural sags that extended upward as high as 2,500 ft (760 m) and influenced sandstone distribution patterns and reservoir compartmentalization in the clastic units of the shallower Bend Conglomerate (Middle Pennsylvanian). This finding is significant, and we now believe that similar karst models could be adopted in many basins where productive clastic reservoirs overlie extensive carbonate sections, particularly if these carbonates have ever been subaerially exposed by uplift and become vadose or high phreatic groundwater zones.

3-D Seismic Program

The 3-D seismic grid at Boonsville field covered approximately 26 mi^2 (67 km^2), starting at the west shore of Lake Bridgeport and extending westward across Wise County and into Jack County. The area covered by the 3-D survey is outlined in the map displayed in Figure 2, which also shows the extensive well control that existed in this active gas field. In addition, this map shows the locations of the wells where VSP and checkshot data were recorded to permit log-defined depths of key sequence boundaries to be converted to accurate two-way time coordinates.

An extensive effort was made to determine the optimal 3-D seismic field procedures that should be used to image the thin-bed reservoirs deposited in the low-accommodation conditions that existed during Middle Pennsylvanian (Atoka) time on this shelf margin of the Fort Worth Basin. This seismic field program involved the following research investigations:

1. Establishing vertical wavetesting as a technique for comparing seismic sources and for selecting the optimal source parameters for imaging U.S. Midcontinent thin-bed reservoirs (Bureau of Economic Geology, 1995a).

2. Verifying the interpretational value of a staggered-source-line, staggered-receiver-line recording geometry that allows 3-D data to be sorted into (a) large bins with high stacking fold or (b) small bins with low stacking fold (Bureau of Economic Geology, 1995b).

3. Documenting the traveltime differences exhibited by explosive sources and swept-frequency sources in U.S. Midcontinent rocks so that vibroseis-source VSP data can be used to calibrate subsurface stratigraphy in 3-D seismic images generated with explosive sources.

4. Demonstrating the economic and technical advantages of using small explosive charges in shallow holes, rather than larger charges in deep holes, as a 3-D seismic energy source in U.S. Midcontinent prospects (Bureau of Economic Geology, 1995c).

Energy Source

On-site inspection of the 3-D seismic area showed that about one-third of the 26-mi^2 (67 km^2) grid was heavily timbered, particularly in the northern and eastern portions abutted to Lake Bridgeport. Vibroseis sources could not be used in these forested areas because permitting restrictions in some properties prohibited clearing vehicle driving lanes through the timber; in other properties, landowners imposed excessive costs for disposing of felled trees. As a consequence, the most logical source to use in these timbered areas was explosives in shot holes, although these shot holes had be prepared by drills that were small enough to wend their way through the timber without having to cut any trees.

The explosive charge selected for wavetesting was the C10 design, composed of 10 oz (285 gm) of high-velocity pentolite molded into a directional charge that focuses the impulsive force downward (Bureau of Economic Geology, 1995c). These charges were planted in holes 10 ft (3 m) deep with the assumption that this hole depth was adequate for good energy coupling but that minimal rifling (i.e., hole blowouts) would occur. During the 3-D seismic data acquisition, sometimes one shot hole (and in a few rare occasions, two) blew out in the five-hole arrays, but the overall negative effect of this reduced energy output for a few shotpoints randomly dispersed throughout the 3-D survey area was minimal. On-site spectral calculations made during a preliminary vertical wavetest showed that these small, shallow, directional charges produced a remarkably broadband signal spectrum with frequencies exceeding 200 Hz measured downhole at the reservoir target depth of 5,000 ft (1,525 m) during vertical wavetesting (Bureau of Economic Geology, 1995a, 1995c). However, the highest signal frequency observed in the surface-recorded field records was approximately 150 Hz.

Staggered-Line Recording Geometry

A 3-D source-receiver geometry, referred to as a staggered-line grid, was implemented at Boonsville field (Bureau of Economic Geology, 1995b). In this geometry, adjacent source lines were shifted by one-half of the source interval, and likewise, adjacent receiver lines were shifted by one-half of the receiver interval. This recording technique allowed the data to be sorted into large, high-fold bins measuring (0.5 × source interval) × (0.5 × receiver interval) or into small, low-fold bins measuring (0.25 × source interval) × (0.25 × receiver interval). In our Boonsville survey, the receiver and source intervals were both 220 ft (67 m), so the sizes of the two stacking-bin options provided by this staggered-line geometry were 110 × 110 ft and 55 × 55 ft (33 × 33 m and 17 × 17 m).

This recording geometry allowed higher fold, large-bin data to be used as the primary data set for determining accurate residual statics and precise stacking velocities and for the initial seismic interpretation; the lower fold, small-bin data were used when greater lateral resolution was needed in the interpretation process. The technical advantage of this staggered-line technique is that the increased lateral resolution it provides is accomplished by directly sorting the data into small bins during the stacking process and not by doing some type of trace interpolation that converts a large trace spacing to a smaller trace spacing. The economic advantage is that small-bin data are acquired at the reduced costs associated with large-bin data acquisition.

Line Spacing and Stacking Fold

The basic field design plan was to space north-south receiver lines 880 ft (270 m) apart and to separate source lines a distance of 1,320 ft (400 m) orthogonal to these receiver lines (that is, east to west). This source-receiver line geometry was surveyed over the 26-mi^2 (67 km^2) 3-D seismic area, except that in some locations the line spacings were varied to avoid production facilities and to minimize cultural problems. The full stacking folds that resulted from this geometry when the data were sorted into 110- × 110-ft (33 × 33 m) bins and then into 55- × 55-ft (17 × 17 m) bins were ~20 and ~5, respectively. These two stacking-fold distributions differed by a factor of 4, as expected, because the respective stacking bin areas differed by a factor of 4.

Recording Aperture

The Atokan-age reservoirs at Boonsville field occur at depths from 4,500 to 6,000 ft (1,370 to 1,830 m), so the 3-D receiver aperture was designed as eight adjacent north-south receiver lines, each 2.5 mi (4 km) long, with the source point being at the center of this rectangular receiver grid. This aperture created a maximum source-receiver offset of 6,600 ft (2,010 m) in the north-south direction and 3,520 ft (1,075 m) in the east-west direction. Ideally, the east-west offset should also have been ~6,000 ft (~1,830 m) (the depth of the deepest reservoir to image), but an aperture of that size was not possible because the data were recorded at a sample rate of 1 ms and a larger number of recording channels would have introduced data transmission problems during data acquisition.

Processing

The Boonsville 3-D data were processed by Trend Technology, Inc., Midland, Texas. Trend imposed stringent processing requirements to preserve the high frequencies that were known to exist from vertical wavetesting (Bureau of Economic Geology, 1995c). Because several field records had a high level of noise contamination due to the presence of several large gas compressor stations and numerous pumping wells, the processing procedures that Trend used produced remarkably good 3-D images of the targeted Atokan thin-bed stratigraphy. The data-processing

technology used to image the thin-bed reservoirs distributed throughout Boonsville field are summarized in Table 1, and the more critical components of this processing procedure are described in the following sections.

Early processing tests demonstrated that wideband reflections did indeed exist in the surface-recorded field records throughout the Atokan interval (approximately 0.8 to 1.0 s) and that these reflection signals contained robust energy spanning a frequency range from about 10 Hz up to as much as 150 Hz in some field records (Hardage et al., 1995). Although the initial goal of preserving the observed downhole frequencies (up to 200 Hz) in the surface-recorded field records was not realized, the signal spectra still had impressive bandwidths that exceeded three octaves.

Static Corrections

Because the Boonsville data contained reflection signals with frequencies exceeding 100 Hz, precise static corrections were essential to preserve the high-frequency components of these signals in the final 3-D images. In addition to correcting the shot and receiver elevations to a uniform depth datum, refraction statics and residual statics were calculated and applied as iterative processes until the time shifts that had to be applied to the traces converged to an acceptably small value. The residual static calculation procedure in Table 1 was a six-stage iteration process. The residual static corrections converged with each iteration, finally reaching the desired objective where no static correction exceeded one time sample (± 1 ms) anywhere inside the 3-D grid.

Velocity Analysis

Velocity analyses are often performed at intervals of approximately 0.5 mi (800 m) across a 3-D seismic grid, and the optimal stacking velocities at these analysis sites are then used to construct an areal velocity map that can be used to stack data at every common depth point (CDP) in the grid. A much more detailed velocity analysis was done at Boonsville field so that the high-frequency portion of the reflection wavefield would be properly time shifted by the velocity moveout corrections before traces were summed at any of the CDP locations.

Specifically, velocity analyses were done along east-west lines separated by only 440 ft (135 m), i.e., along every fourth row of the 110- × 110-ft stacking bins inside the 3-D grid. Within each of these east-west lines, a velocity analysis was done using 50 different velocity functions at every CDP, not at CDP's spaced 0.25 or 0.5 mi apart, as is often done. As a consequence, approximately 850,000 velocity panels were created across the Boonsville 3-D survey area, which is about two orders of magnitude more velocity information than is often used to determine stacking velocities. This intense velocity analysis did not require an excessive amount of calendar time because the data processing contractor implemented an effective, automated calculation procedure.

Data Interpretation

One unique aspect of the Fort Worth Basin stratigraphy that was revealed by the 3-D seismic images created in this study was the manner in which Atokan-age (Middle Pennsylvanian) sedimentation had been influenced by solution collapse that originated in deep, Ordovician-age Paleozoic carbonate rocks. Although there were hints from well control that small grabenlike structural features could be present in the basin, neither the vertical displacements nor the fault-block geometries could be mapped accurately without 3-D seismic data. This karsting phenomenon can be illustrated by inspecting seismic-derived structure maps traversing the base and top of the Bend Conglomerate interval. Time structure maps produced during the course of the Boonsville 3-D seismic interpretation are presented as Figures 3 and 4 and show, respectively, the topography at the top of the Bend Conglomerate (or the Caddo surface) and the topography near the base of the Bend Conglomerate (or the Vineyard surface).

Inspection of the Vineyard structure map (Fig. 4) shows that several depressions occur in a seemingly random pattern across the Vineyard chronostratigraphic surface. These depressions tend to have circular to oval shapes, with diameters ranging from about 500 (150 m) to about 3,000 ft (915 m). Groups of karst collapse features sometimes occur along linear northwest-southeast trends, suggesting some type of a genetic relationship between these structural depressions and basement faults (Fig. 3).

Inside the 3-D seismic grid, well log control defined the Caddo surface (top of the Bend Conglomerate) to be 1,000 to 1,200 ft (305 to 365 m) above the Vineyard surface (basal unit of the Bend Conglomerate). The seismic-interpreted Caddo surface developed in this study is displayed in Figure 3. This map shows that depressions similar to those at the Vineyard level also occur across the Caddo surface. An important observation is that these Caddo depressions, particularly the three prominent ones labels 1, 2, and 3, are positioned directly above equivalent depressions in the Vineyard surface approximately 1,000 ft (305 m) deeper, implying that there is a genetic relationship between the Caddo depressions and the older Vineyard depressions.

The seismic reflection response inside each of these structural depressions differs significantly from the reflection response in unaffected areas. This variation in seismic reflection behavior is documented in our data when the reflection response is displayed across an interpreted chronostratigraphic surface. One example of the seismic reflection sensitivity to these surface depressions is shown in Figure 5, which is a display of the reflection amplitude magnitude on the Vineyard time structure surface. Because this chronostratigraphic surface was interpreted so that it followed the apex of a reflection trough, the reflection amplitudes on the surface have the same negative algebraic sign but variable magnitudes; exceptions being that some positive values occur in small, local areas where the chronostratigraphic surface had to phantom through zones that were characterized by distorted and variable reflection waveshapes. When the seismic wiggle trace data corresponding to this Vineyard chronostratigraphic surface are displayed so that all positive reflection amplitudes are one color and all negative reflection amplitudes are a different color, as is done in Figure 5, the reflection amplitude map should have the same color, but with varying intensity, across the entire surface, except in the several local areas where the Vineyard reflection becomes distorted or exhibits a low signal-to-noise character and random polarity changes.

Inspection of this map shows that quasi-circular disruptions (appearing as white areas) occur across this seismic amplitude response map, and correlating this disruption pattern with the Vineyard structure map (Fig. 4) confirms that each of these dramatic alternations in the seismic reflection response corresponds to a depression in the Vineyard surface topography.

The location of profile ABC shown in Figure 5 was chosen so that it traversed three of these seismic reflection anomalies on the Vineyard surface: a rather large anomalous area between A and B and two smaller, circular anomalies between B and C. A section view of the seismic behavior along this profile is provided as Figure 6, and in this view the consistently near-vertical attitude and the extreme height of these stratigraphic disruptions are striking. Each structural disruption begins at seismic basement (not far below 1.2 s), which is the Ellenburger Group (Ordovician age), and extends vertically into, or completely through, the Bend Conglomerate clastics (Pennsylvanian Atokan age), causing the vertical extent of these disrupted zones to be as much as 2,000 to 2,500 ft (610 to 760 m) throughout the Boonsville 3-D seismic grid. In a few instances, a disruption continues into the Strawn section above the Bend Conglomerate.

These structural collapse zones occur at a rather high spatial density, with adjacent collapses often separated by only 1 mi (1,600 m) or less (see Fig. 5), and as noted, each zone extends completely through the Pennsylvanian-age Bend Conglomerate, or at least through a significant part of the Bend Conglomerate interval. Because of the severe stratigraphic disruption that these collapses cause within the Pennsylvanian section, some of these basement-related collapses were a significant influence on Pennsylvanian and Mississippian sedimentation, and thus these basement-related phenomena need to be considered when evaluating any prospects in basins underlain by karst-prone carbonates. For example, Sanders and Steel (1982) used 3-D seismic data to document that karst features much like these we have observed occur in the Gippsland basin, offshore southeastern Australia. Examples of these features from the Gippsland basin are included in the widely circulated AAPG Memoir 42 (Brown, 1991).

Geological Mechanism for Collapse Structures

These extensive vertical collapse zones are interpreted to be the result of post-Ellenburger carbonate solution weathering, which occurred during periods of subaerial exposure. Lucia (1995) discusses the time occurrences and time durations of these subaerial exposures of Ellenburger rocks; his analysis will not be repeated here. This karst model is adopted because karst-generated vertical collapse zones can be observed in Ellenburger outcrops in the Franklin Mountains at El Paso, Texas, and because Ellenburger karst plays are pursued by some operators in the Permian Basin of West Texas. In the Franklin Mountains outcrops, the measured lateral dimensions of the collapsed features correspond to the diameters of several of the disrupted zones observed in the 3-D seismic image at Boonsville (Fig. 7). The outcrop features also have extensive vertical dimensions, as do the seismically imaged collapses at Boonsville, with some of these outcrop collapses extending vertically for at least 1,200 ft (365 m) in the larger outcrop exposures (Fig. 7).

It is important to note that the Ellenburger karst collapse zones observed in outcrops in the Franklin Mountains and the Ellenburger-related collapse zones observed in our Boonsville 3-D data

in the Fort Worth Basin document that this Paleozoic karsting phenomenon spans a distance of at least 500 mi (800 km). The influence of this deep karst collapse on younger sedimentation needs to be studied at several sites between these two widely separated control points (El Paso to Wichita Falls) to better document how this karsting phenomenon affects hydrocarbon production and exploration strategy throughout the Permian and Delaware Basins of West Texas.

Although no Ellenburger cores are available within the Boonsville project area, these regional outcrop observations and the Boonsville seismic images allow the following karst-related hypothesis to be put forward regarding the genesis of the Boonsville collapse structures:

1. Post-Ellenburger/pre-Bend Conglomerate basement faulting (apparently strike-slip(?) faults trending north-northwest) occurred across the area of Boonsville gas field.

2. Karst solution weathering then occurred, particularly along vertical fractures related to northwest trending faults where water seepage was enhanced, and this process produced large caverns in some carbonate units.

3. As Mississippian and Pennsylvanian sediment accumulated, sediment loading caused these karst-induced caverns to collapse. Lucia's (1995) field observations in the Franklin Mountains imply that collapse often occurred when approximately 2,000 ft (610 m) of overburden accumulated.

4. The presence of the resultant collapse structures influenced the distribution of sandstone reservoir facies within the various Atokan sequences. Periods of active collapse would have produced a hilly, hummocky physiography, and downcutting fluvial systems would occupy these subtle, collapsed areas, allowing site-preferential aggradation of high-energy, active-fluvial, and deltaic facies.

5. The locations of active collapsing apparently varied with time and caused each Bend Conglomerate genetic sequence in our study area to be affected differently.

6. Episodes of collapse probably continued until the majority of the solution caverns had collapsed and filled from above, resulting in displacement of overlying strata. Lucia's (1995) field measurements show that the structural sag in the overlying strata is usually of the order of 40 to
60 ft (12 to 18 m).

Reservoir Compartmentalization Resulting from Karst Collapse Processes

One example of deep-seated karst collpase that created reservoir compartmentalization at the Caddo level, some 2,500 ft (760 m) above the Ellenburger and in much younger, Atokan-age clastic rocks, is the situation associated with the Sealy C-2 well in the northeast quadrant of our 26-mi^2 (67-km^2) 3-D seismic study area (Fig. 2).

The Sealy C-2 was spudded in September 1992 and drilled through the basal Bend Conglomerate to a total depth of 5,830 ft (1,777 m). The pressures measured in the Upper Caddo were higher than expected and suggested only partial pressure depletion in this interval.

The Upper Caddo was perforated from 4,886 to 4,902 ft (1,489 to 1,494 m) and treated with 2,000 gal of 15 percent HCl. Following cleanup of the acid treatment, a pressure buildup test was conducted, and an average reservoir pressure of 1,300 psi was estimated for the Upper Caddo. Following the shut-in period, the Sealy C-2 produced at a rate of 1.04 MMscf/d during a 24-h flow test.

Figure 8 is a plot of initial pressures in the Upper Caddo measured from wells in the project area over time. The value of initial pressure for the Sealy C-2 well is similar to those reported in wells drilled and completed in the 1950's. Note that in each case the pressures reported are the best estimates that could be obtained for particular wells using available data sources (both operator and public domain records). The estimated initial reservoir pressure for the Sealy C-2 of 1,300 psi represented a pressure gradient of about 0.3 psi/ft (1 psi/m). This pressure suggested that the Sealy C-2 location had been partially drained by surrounding production, although the pressure was higher than would be expected, given the extent of the offsetting production from the Upper Caddo. It should be noted that this Caddo reservoir is in an underpressured sequence and that the original pressure gradient is of the order of only 0.35 to 0.4 psi/ft.

The northeast quadrant of the Caddo time structure map (Fig. 3) is enlarged in Figure 9, and the locations of the Sealy C-2 and several neighboring wells are identified. This map shows that the Sealy C-2 well was drilled on what appears to be a structural high. However, when the structural and stratigraphic details associated with the Sealy C-2 well are viewed in seismic section views along lines A, B, C, or D (Fig. 9), it is apparent that the well is not positioned on a structural high created by tectonic uplift, but rather it is on a portion of the Caddo surface where the terrain surrounding the well collapsed because of underlying Ellenburger-related karsting.

Lines A, B, C, and D are presented as Figure 10 to support this karst compartmentalization model. All profiles show that vertical, seismically disrupted, collapse zones extend from the Ellenburger (approximately 1.2 s) up to the Caddo and that these collapse zones completely surround the Sealy C-2 well. These vertical seismic sections indicate that numerous low-displacement, vertical faults (often with throws of only 20 to 30 ft [6 to 9 m]) separate the Sealy C-2 well from the surrounding terrain, the same order of structural collapse observed in outcrop studies by Lucia (1995). The estimated Upper Caddo reservoir pressure of 1,300 psi encountered in the C-2 well and the subsequent production history (Fig. 11) suggest that these low-displacement faults acted as partial barriers to fluid flow at the Caddo level. The area inside the circumference defined by this ring of collapse is approximately 130 acres; thus, if it is assumed that the karst collapse zones are partial flow barriers, then the Sealy C-2 well is producing from a Caddo reservoir compartment spanning about 130 acres.

Figure 11 shows the actual production from the Sealy C-2 well. This is a log-log plot of gas flow rate versus time. The well came on line in November 1992 and produced 800 to 900 Mscf/d for the first couple of months. Since then, the gas flow rate has gradually declined to about 200 Mscf/d after just over 2 yr of production, and the well has produced about 350 MMscf of gas

to date. The production data, when plotted this way, show the influence of reservoir boundaries, as evidenced by the concave downward shape of the later-time data.

The production data were history-matched with an analytical reservoir model to estimate reservoir properties and gas in place. As Figure 11 shows, the analytical model provides a good match of the actual production data. From this analysis, a permeability of 2.2 md, a skin factor of –2 (indicating slight stimulation following the acid treatment), and a drainage area of 128 acres were determined. The estimated reservoir area of 128 acres agrees well with the 130-acre reservoir size identified from the seismic interpretation, as described previously.

Using this reservoir description, future performance of the Sealy C-2 was projected. The Sealy C-2 is expected to recover another 200 MMscf over the next several years, resulting in an ultimate gas recovery of about 550 MMscf. This projected ultimate recovery is at the high end of what might be expected statistically from an Upper Caddo gas completion in the project area. In addition, this projected future recovery is for the Upper Caddo reservoir only; there still appear to be behind-pipe opportunities in other Bend Conglomerate sequences, which may lead to additional gas recovery from this well.

We emphasize that the reservoir size estimated from the production data analysis was essentially the same as that predicted from the 3-D seismic interpretation. The reservoir performance supports the seismic interpretation concept of an Upper Caddo reservoir compartment created by Ellenburger karst-collapse zones that surround the Sealy C-2 well. None of the reservoir pressures measured in the Bend Conglomerate intervals from the Caddo through the Vineyard, however, could be considered initial reservoir pressures; all indicated varying degrees of pressure depletion at this location. Therefore, the low-displacement faults associated with these karst collapse features seem to act as partial, not total, barriers to gas flow in this case. The degree of reservoir isolation caused by this low-scale faulting appears to vary from sequence to sequence through the Bend Conglomerate interval.

In May 1995, the Sealy C-3 well was drilled approximately 1,500 ft (460 m) northeast of the Sealy C-2 location (Figs. 2 and 9) on the same karst-isolated Bend Conglomerate section as the C-2 well. A pressure of 1,005 psi was measured in the Upper Caddo, indicating that this new well penetrated the same reservoir compartment as the older C-2 well. This pressure measurement supports the seismic interpretation that the Ellenburger karst-generated structural feature in Figure 9 created an Upper Caddo reservoir compartment because that pressure value agrees with what should exist within the reservoir at this location given the size of the structure (compartment), the two well locations within the compartment, and the total production (degree of depletion) from the Sealy C-2 well.

A second confirmation that this karst-isolated feature created distinct reservoir compartments was that the Sealy C-3 well penetrated a second gas-bearing sand near the base of the Bend Conglomerate interval. Pressures of 2,196 and 2,200 psi were measured in this reservoir during two tests, which are initial pressures at that particular reservoir depth. Thus, the Sealy C-3 well encountered a previously undrained compartment, which was isolated from laterally equivalent reservoirs in the same genetic sequence. This reservoir isolation is again suggestive

evidence that the deep-origin, karst-generated, stratigraphic disruption that surrounds the C-3 well location has compartmented a clastic section far above the onset of the karsting phenomena.

Initially, this deeper reservoir tested 3 MMscf per day at 1,500 psi flowing tubing pressure (FTP); it was making more than 1 MMscf per day at about 1,600 psi FTP after one month of production. We will continue to monitor the performance of the Sealy C-3 well to determine the effective size of this deeper reservoir. Although this productive sandstone was not present in the C-2 well, if the reservoir facies should cover the greater part of the structure illustrated in Figure 9, the gas reserves associated with this reservoir could be in excess of 500 MMscf. The discovery of this second isolated reservoir in the Sealy C-3 well further illustrates the influence of Ellenburger karst collapse features on younger stratigraphy, on potential reservoir compartmentalization in the Bend Conglomerate section of the Fort Worth Basin, and, by inference, on stratigraphy and compartmentalization in other basins that are underlain by carbonate sections.

Buried Statics—An Alternative Explanation?

As a part of the official technology transfer phase of this SGR project, we have presented this 3-D seismic interpretation story to several hundred oil and gas operators in Texas and surrounding states, and during one of these short courses, one challenge to our karst model was raised, that being that the vertical disruptions seen in the 3-D seismic images are caused by buried statics and are not vertical karst-collapse chimneys. Our position is that the seismic disruptions are related to deep Ellenburger karsts, not to buried statics, for the following reasons:

1. The Bend Conglomerate section consists of hard, competent, well-consolidated, high-velocity rocks. We have difficulty visualizing what mechanism can cause buried statics in such a rock system at depths of 4,500 ft (1,370 m) and more.

2. The physical dimensions of the observed seismic disruptions agree with the heights and diameters of Ellenburger-generated karsts observed in Franklin Mountains outcrops, as do the magnitudes of the structural sags produced in the overlying strata (Lucia, 1995).

3. The karst halo phenomenon proposed in Figure 9 is supported by the Caddo reservoir size inferred from the Sealy C-2 production history (Fig. 11).

4. The discovery of a deeper, isolated reservoir in the Sealy C-3 well (Fig. 9) near the base of the Bend Conglomerate confirms that the stratigraphic disruption surrounding that well extends vertically almost 1,000 ft (300 m). This fact supports a vertical karst-collapse chimney, not a static time shift localized at the top of the Bend Conglomerate section.

5. Most of the seismic disruptions align along linear trends that do not coincide with the orientation of east-west source lines and north-south receiver lines (Fig. 5). This behavior suggests a genetic relationship to basement faults, and the vertical fractures

associated with faults are often the conduits by which fluids reach carbonate sections and produce karsts.

6. The amount of vertical disruption (sag) consistently decreases upward in the section, as do breccia pipe collapses observed in outcrop.

It is not straightforward as to what data processing tests will confirm that buried statics exist. Some processors have suggested that a logical test would be to create two stacked data volumes—one stack dominated by short-offset data and the other based on long-offset data—and to compare the structures produced in these two images. A significant structural difference might suggest that buried statics exist. We approximated this test by creating two stacked data volumes—one volume being a low-fold, small-bin stack and the second being a high-fold, large-bin stack. We observed no significant structural differences in these two 3-D images. Also, in our experience, buried statics produce obvious V-shaped anomalies in stacked images; we observe no such anomalies in our data stacks.

A more rigorous test that should indicate if buried statics caused the observed reflection disruptions would be to create earth models that define the depth, areal size, and vertical extent of hypothetical static-affected rock volumes, then ray trace model the arrival times that should be observed when the actual source-receiver geometry is deployed over these models and compare these ray trace times with the arrival times observed in the field records. These 3-D ray tracing tests have not been done.

Conclusions

There are approximately 200 wells inside the 26-mi^2 (67 km^2) area we studied, which is rather good subsurface control. Yet even with this drilling density, few, if any, operators in the area were aware that the Ellenburger-related karst phenomena described here existed in Boonsville field. We are convinced that if we had relied strictly on well control, we too would not have recognized how seriously deep karsting affected shallower Pennsylvanian clastic stratigraphy and Boonsville gas production. Our experience tells us that operators in similar carbonate-prone basins must acquire 3-D seismic data to fully evaluate karst effects. However, once 3-D seismic data are acquired, we believe (and strongly recommend) that extensive geologic and reservoir engineering data bases be created to properly interpret the 3-D seismic images and that good-quality VSP data be acquired to allow these geologic and engineering controls to be inserted into the 3-D seismic image at the correct two-way time coordinates.

Because we know that Ellenburger solution-collapse phenomena span a distance of at least 500 mi (800 km) from our study area in the Fort Worth Basin to the Ellenburger outcrops in the Franklin Mountains at El Paso, Texas, karst phenomena must affect stratigraphy and reservoir compartmentalization over a vast area of rich hydrocarbon reservoirs in the Permian and Delaware Basins of West Texas. Private discussions with numerous companies who are industry research partners with the Bureau of Economic Geology in worldwide reservoir studies have convinced us that similar karst effects exist in many carbonate-prone basins around the world.

Several fundamental research questions remain to be answered, with some of the obvious issues that need to be addressed being the following:

1. Should wells be positioned inside or outside karst collapse zones?

2. How does a karst extend through an extensive clastic section such as the Bend Conglomerate? Does the collapse occur as episodic events or as a single, catastrophic event?

3. What is the genetic relationship between karsts and faults and what causes the collapse features we observe to be almost perfectly vertical?

Currently, we have only speculative answers to these questions. Both the drill bit and the coring bit will continue to provide valuable information on these intriguing karst phenomena, and we are convinced that 3-D seismic data will be critical in any such future investigations.

Acknowledgments

This work was funded by the U.S. Department of Energy and the Gas Research Institute as a part of the Secondary Gas Recovery project with funding provided by contracts DE-FG21-88MC25031 and GRI-5093-212-2630. We thank Arch Petroleum, Enserch, and OXY USA, Inc., for allowing access to the study area and for providing financial and technical support for the data collection and analysis. The 3-D seismic interpretation was done with software provided by Landmark and workstation hardware provided by IBM. Publication was authorized by the Director, Bureau of Economic Geology, The University of Texas at Austin. This paper was originally published in Geophysics (1996, v. 61, no. 5, p. 1336–1350).

References

Brown, A. R., 1991, Interpretation of 3-dimensional seismic data: AAPG Memoir 42, American Association of Petroleum Geology, Tulsa, OK, 341 p.

Bureau of Economic Geology, 1995a, Vertical wavetesting: The University of Texas at Austin, Bureau of Economic Geology, technical summary of research conducted for the Gas Research Institute, U.S. Department of Energy, and State of Texas, GRI-94/0447, 14 p. (Available as a public education brochure from the Bureau of Economic Geology; telephone 512-471-1534.)

Bureau of Economic Geology, 1995b, Staggered-line 3-D seismic recording: The University of Texas at Austin, Bureau of Economic Geology, technical summary of research conducted for the Gas Research Institute, U.S. Department of Energy, and State of Texas, GRI-

94/0446, 11 p. (Available as a public education brochure from the Bureau of Economic Geology; telephone 512-471-1534.)

Bureau of Economic Geology, 1995c, The use of small, directionally focused charges as a 3-D seismic energy source: The University of Texas at Austin, Bureau of Economic Geology, technical summary of research conducted for the Gas Research Institute, U.S. Department of Energy, and State of Texas, GRI-94/0448, 10 p. (Available as a public education brochure from the Bureau of Economic Geology; telephone 512-471-1534.)

Hardage, B. A., Levey, R. A., Pendelton, V. M., Simmons, J. L., Jr., and Edson, R., 1994, A 3-D seismic case history evaluating fluvially deposited thin-bed reservoirs in a gas-producing property: Geophysics, 59, 1650–1665.

Hardage, B. A., Carr, D. L., Finley, R. J., Lancaster, D. E., Elphick, R. Y., and Ballard, J. R., 1995, Secondary natural gas recovery-targeted applications for infield reserve growth in midcontinent reservoirs, Boonsville Field, Fort Worth Basin, Texas: Topical Report GRI-95/0454, available from the Gas Research Institute, Chicago, IL, or the Bureau of Economic Geology, Austin, Texas.

Lucia, F. J., 1995, Lower Paleozoic cavern development, collapse, and dolomitization, Franklin Mountains, El Paso, Texas *in* Unconformities and Porosity in Carbonate Strata edited by D. A. Budd, A. H. Saller, and P. M. Harris, AAPG Memoir 63, p. 279–300.

Sanders, J. I., and Steel, G., 1982, Improved structural resolution from 3D surveys in Australia: Australian Petroleum Exploration Association (APEA) Journal, v. 22, p. 17–41.

Thompson, D. M., 1982, Atoka Group (Lower to Middle Pennsylvanian), northern Fort Worth Basin, Texas: terrigenous depositional systems, diagenesis, and reservoir distribution and quality: The University of Texas at Austin, Bureau of Economic Geology Report of Investigations No. 125, 62 p.

Table 1. Boonsville 3-D seismic processing sequence.

(1) Surface and Subsurface Maps
(2) Geometry Definition and Application
(3) Prefilter 17-250 Hz
(4) Surface-Consistent Deconvolution
(5) Refraction Statics: Datum = 900 ft, Velocity = 8000 ft/s
(6) Velocity Analysis
(7) Refraction Statics: Datum = 900 ft, Velocity = 8000 ft/s
(8) CDP Stack
(9) Automatic Residual Statics: Iterate 6 Times
(10) Velocity Analysis
(11) Normal Moveout
(12) Spectral Balance
(13) CDP Residual Statics
(14) CDP Stack (55- and 110-ft bins)
(15) Interpolate Missing CDP's at edges of data volume (55-ft bins only)
(16) 3-D Migration

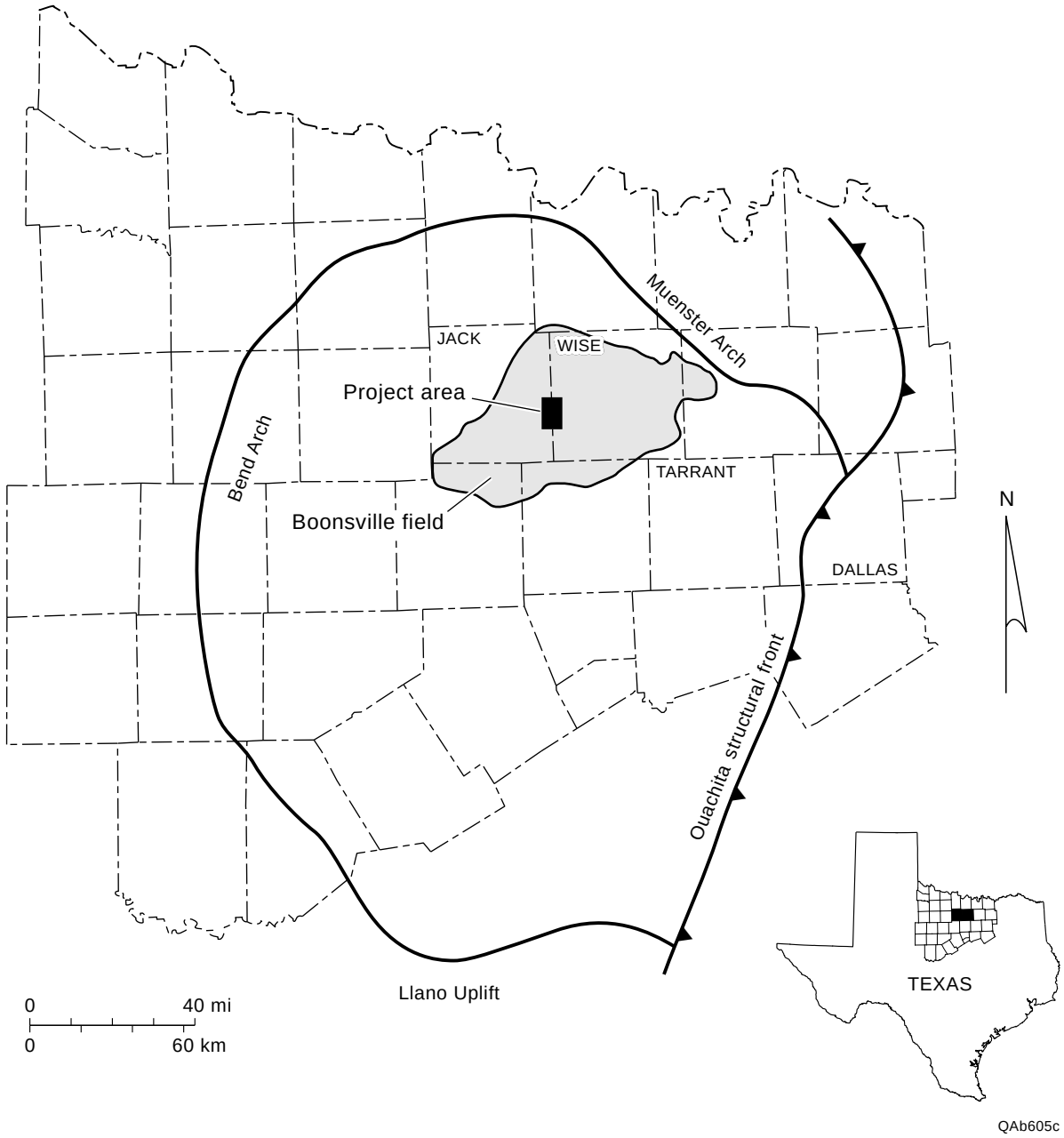

Figure 1. Generalized map of the Fort Worth Basin, Boonsville Field, and project study area. The Fort Worth Basin is bounded on the east by the Ouachita structural front, on the south by the Llano Uplift, on the west by the Bend Arch, and on the north by the Muenster Arch. Boonsville (Bend Conglomerate gas) Field is a large gas field located mostly in Jack and Wise Counties. Our study was concentrated in a 26-mi^2 (67-km^2) area centered on the Jack-Wise county line.

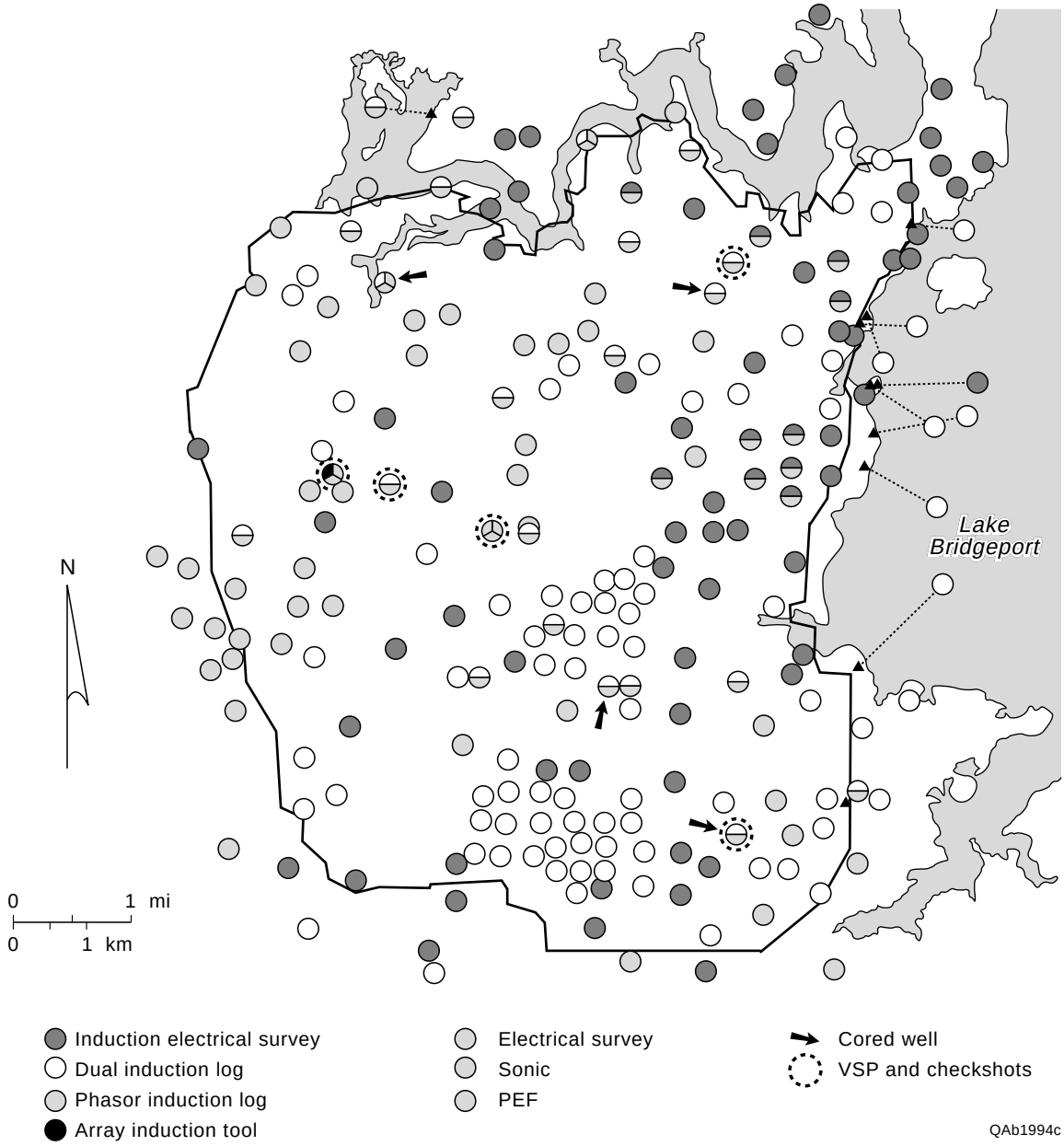

Figure 2. Well control within the study area. The solid line outlines the area wher 26-mi^2 (67 km^2) of 3-D seismic data were recorded. VSP and checkshot data were recorded at five well locations to accurately convert the log-defined depths of key sequence boundaries to accurate seismic two-way coordinates. The Sealy C-2 well that is discussed in Figures 8 through 11 is the cored well in the northeast corner of the study area; the Sealy C-3 well is the checkshot well immediately northeast of the Sealy C-2.

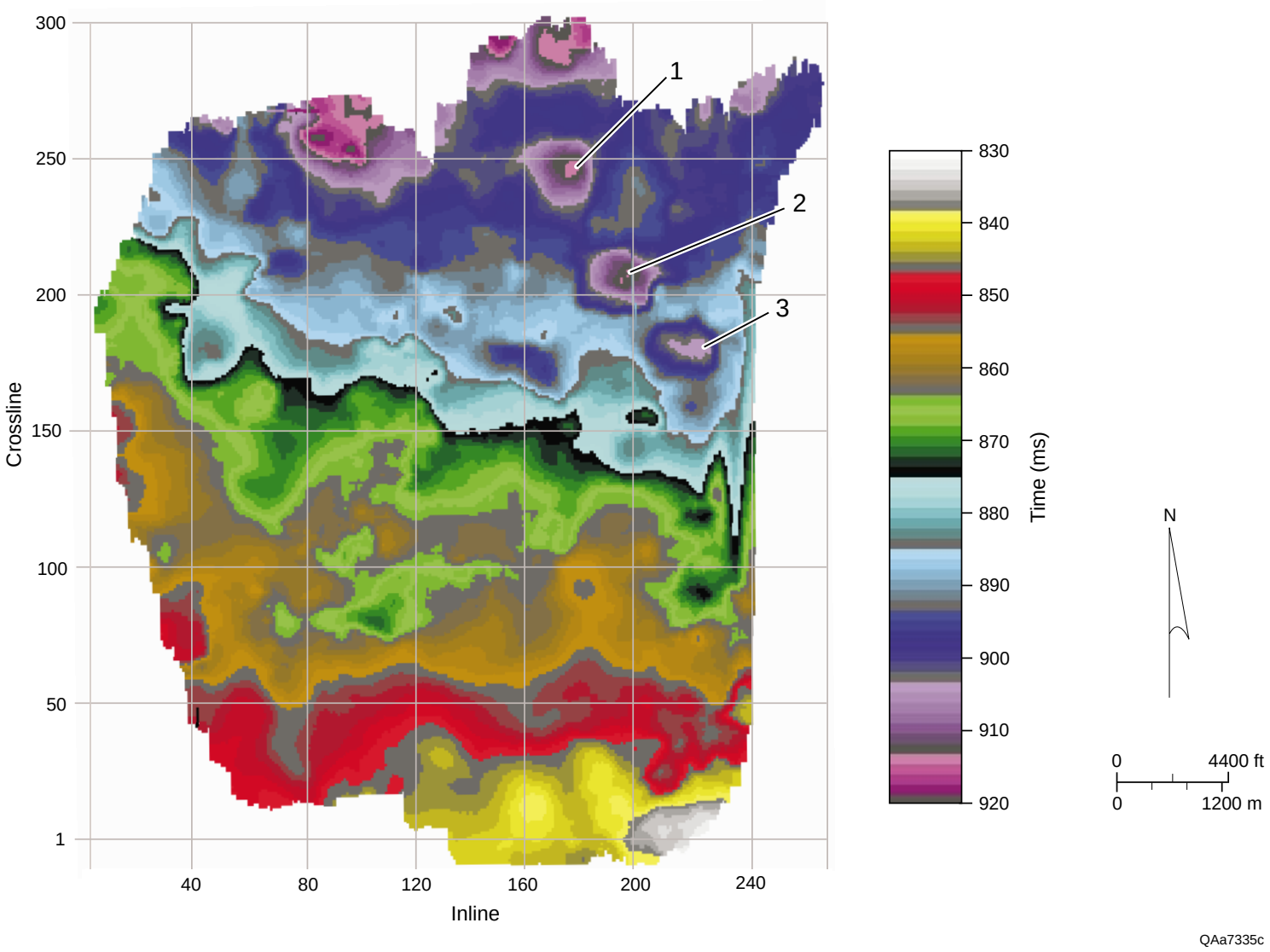

Figure 3. Interpreted time structure map for the top of Caddo, which is the sequence at the top of the productive Bend Conglomerate section. Features 1, 2, and 3 are circular depressions on this surface. Note that these three depressions follow a northwest-southeast linear trend, an alignment along a deeper basement fault.

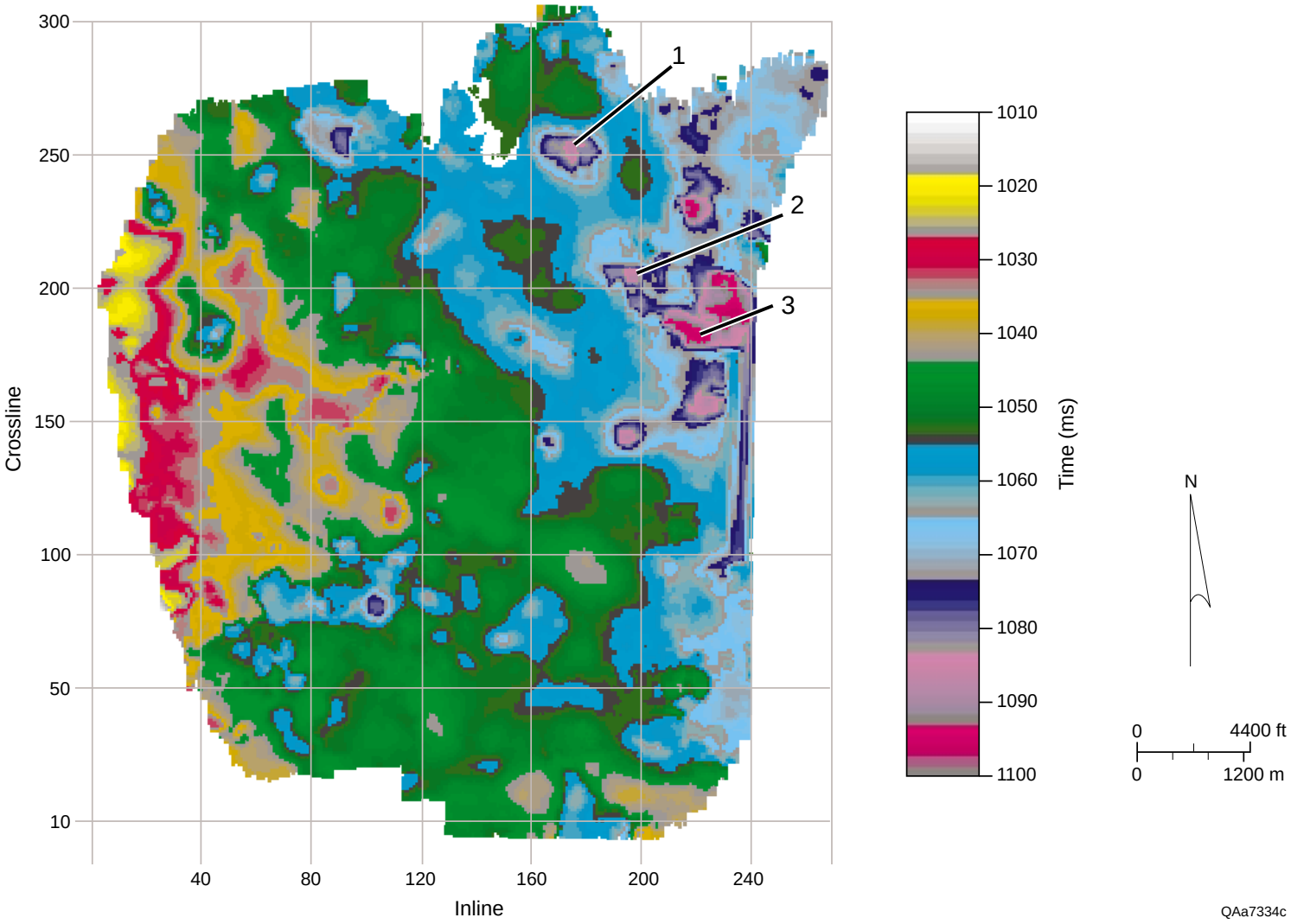

Figure 4. Interpreted time structure map for the top of Vineyard, which forms a sequence near the base of the Bend Conglomerate section. Many more depressions occur on this deeper surface than on the Caddo surface (Figure 3), some 1000 ft (305 m) above the Vineyard. The depressions numbered 1, 2, 3 are positioned directly below depressions 1, 2, 3 observed on the Caddo surface (Figure 3), implying that there is a genetic relationship between the two sets of depressions. Note that most of the structural elements align in a northwest-southeast orientation.

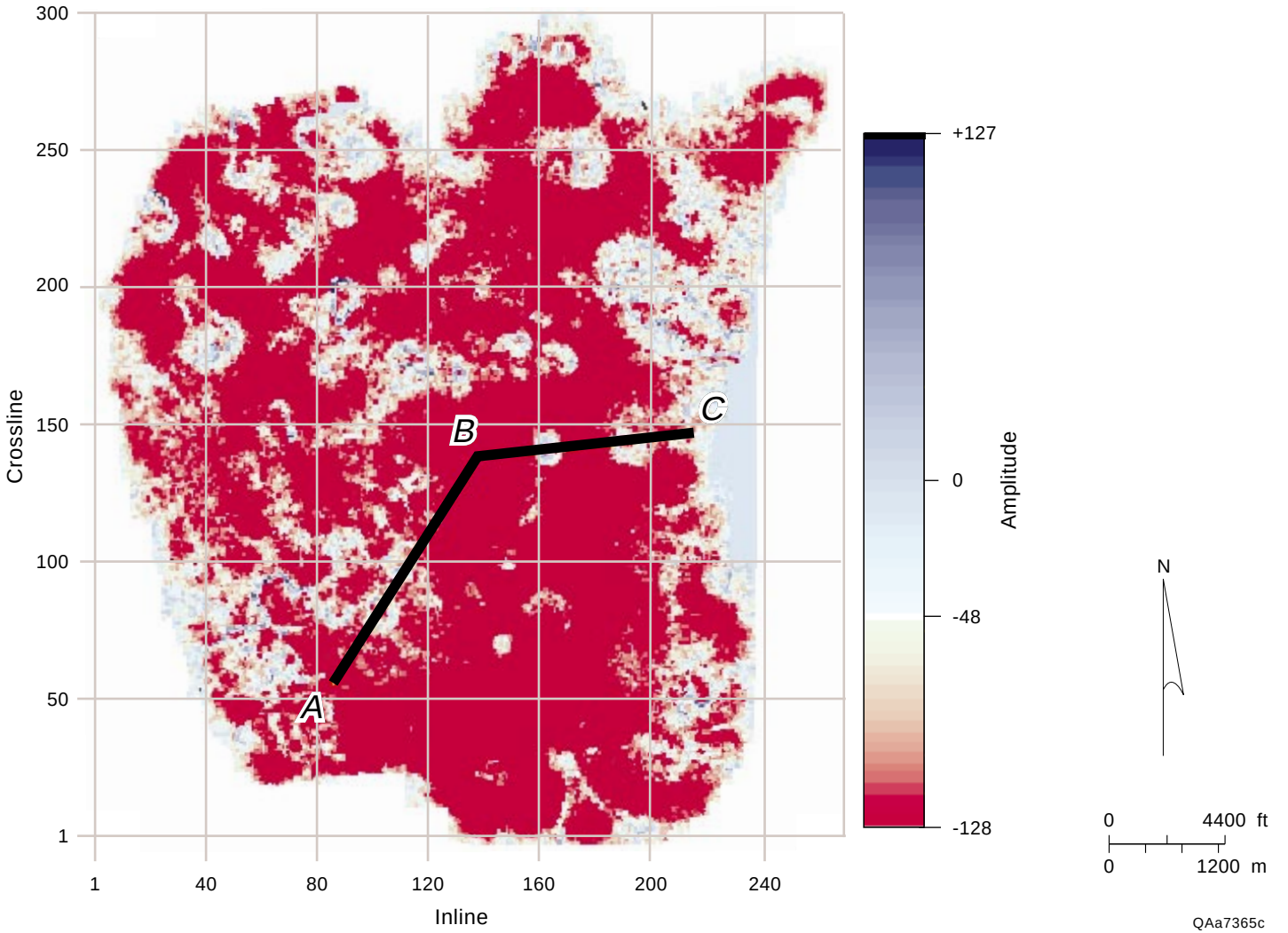

Figure 5. Seismic reflection amplitude response across the Vineyard surface. From well control, this surface was interpreted as a consistent reflection trough; thus, the surface should exhibit a continuous red shade with this choice of color bar. The white and light-blue areas, many of which are nearly circular, indicate where the reflection character is disrupted and the reflection amplitude dims or changes polarity in a random manner. Profile ABC is chosen so that it traverses a sizable disruption midway between A and B and two small, circular disruptions between B and C. Each of these disruptions in the Vineyard reflection character coincides with a depression in the time surface in Figure 4. These disrupted areas tend to align northwest-southeast.

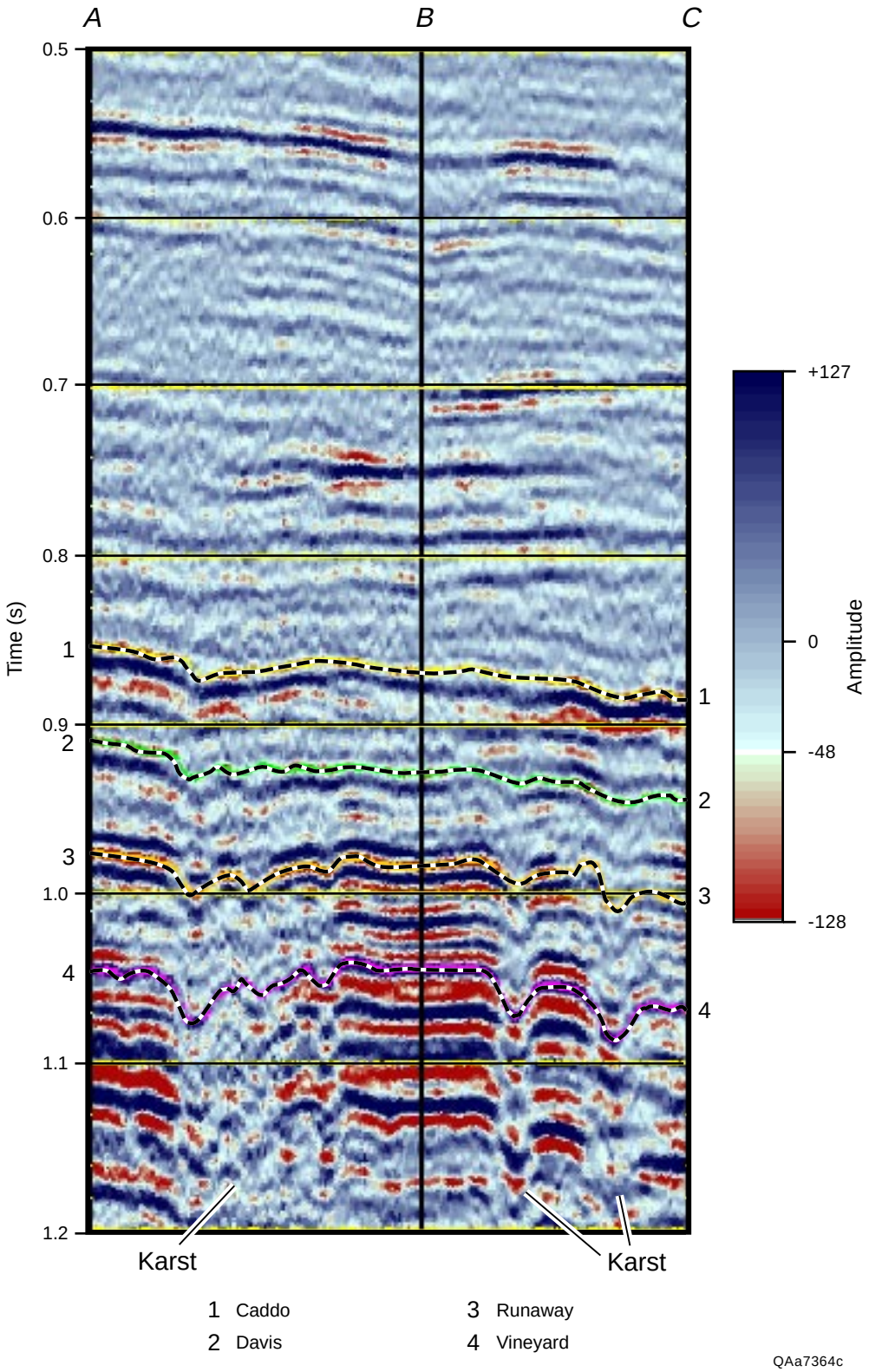

Figure 6. Seismic profile along line ABC, which traverses three of the disrupted zones (white areas) on the Vineyard reflection amplitude surface. Note each disrupted zone extends vertically from seismic basement (slightly below 1.2 s) up to the Caddo level (horizon #1), which is a height of more than 2000 ft (610 m). These collapsed zones are assumed to be genetically related to post-Ellenburger karsting.

a)

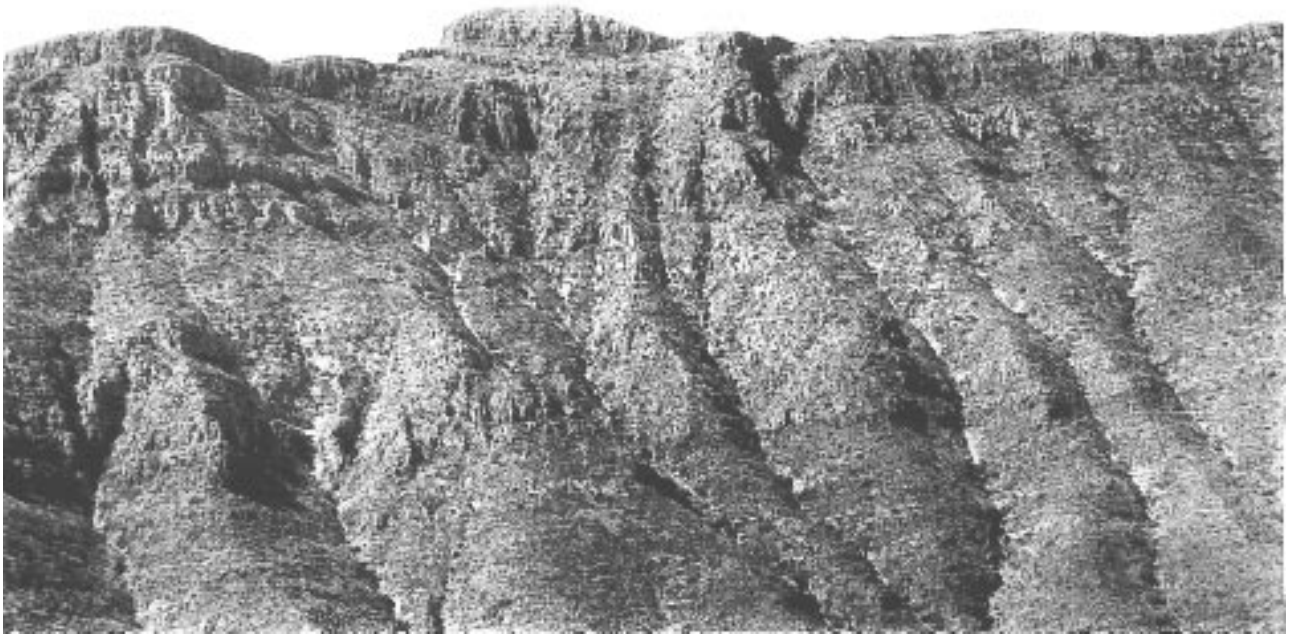

QAb2010(a)c

0 350 ft
0 100 m
Scale is approximate

b)

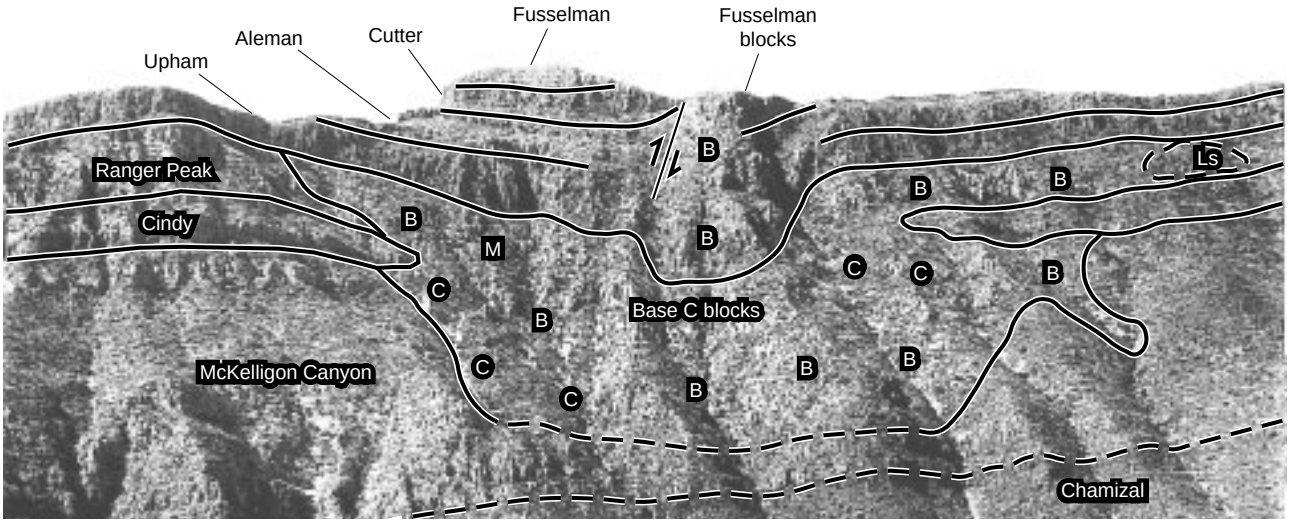

QAb2010c

0 350 ft
0 100 m
Scale is approximate

Figure 7. (a) Uninterpreted photograph of The Great McKelligon Sag (Lucia, 1995). (b) Interpreted photograph of The Great McKelligon Sag in McKelligon Canyon along the east face of the southern Franklin Mountains, showing the distribution of collapse breccia and the collapse of the Ordovician Montoya Group into the Ranger Peak Formation. B = breccia, C = blocks of Cindy Formation, M = blocks of Montoya Group (Lucia, 1995).

c)

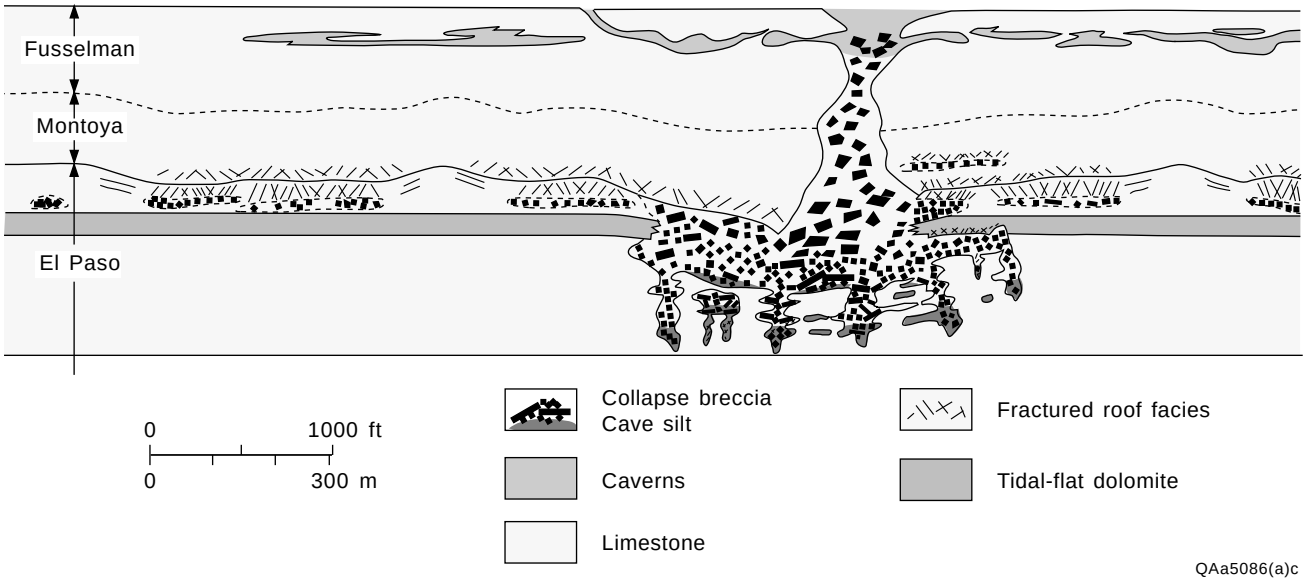

Figure 7. (c) Outcrop mapping and diagram of the El Paso caverns showing collapse of the Ordovician Montoya, development of breccia pipes up into the Silurian Fusselman Formation, and development of caverns in the Fusselman Formation (Lucia, 1995)

d)

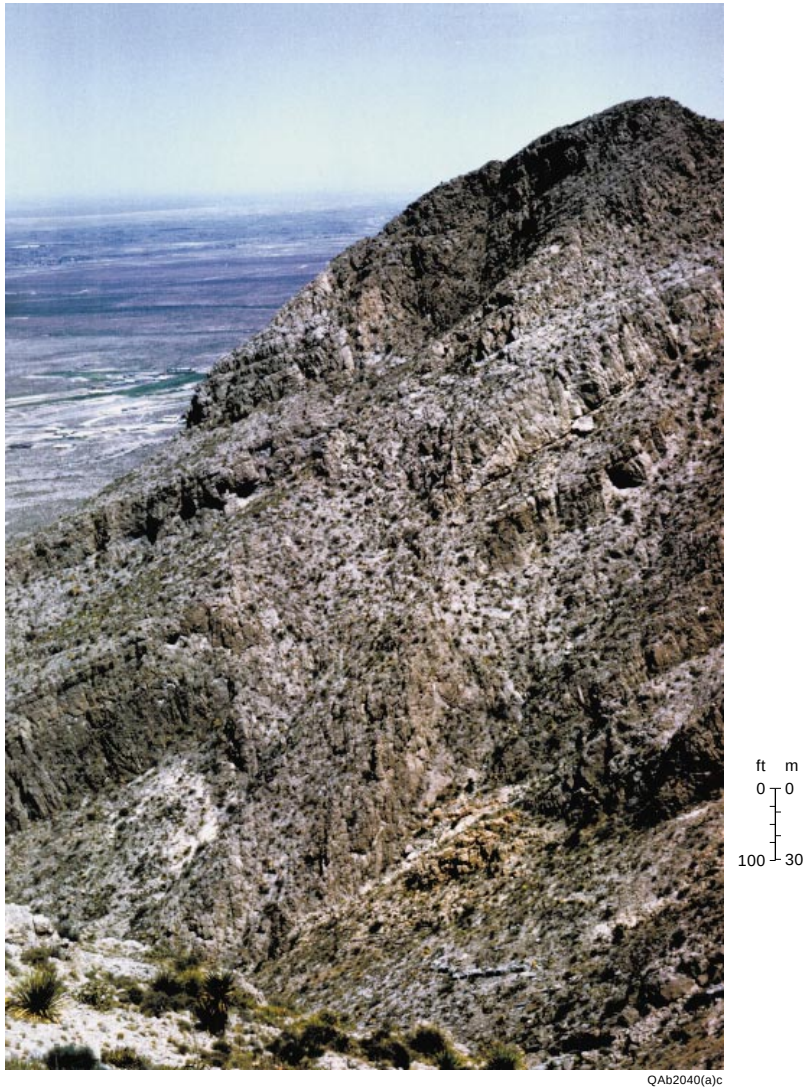

e)

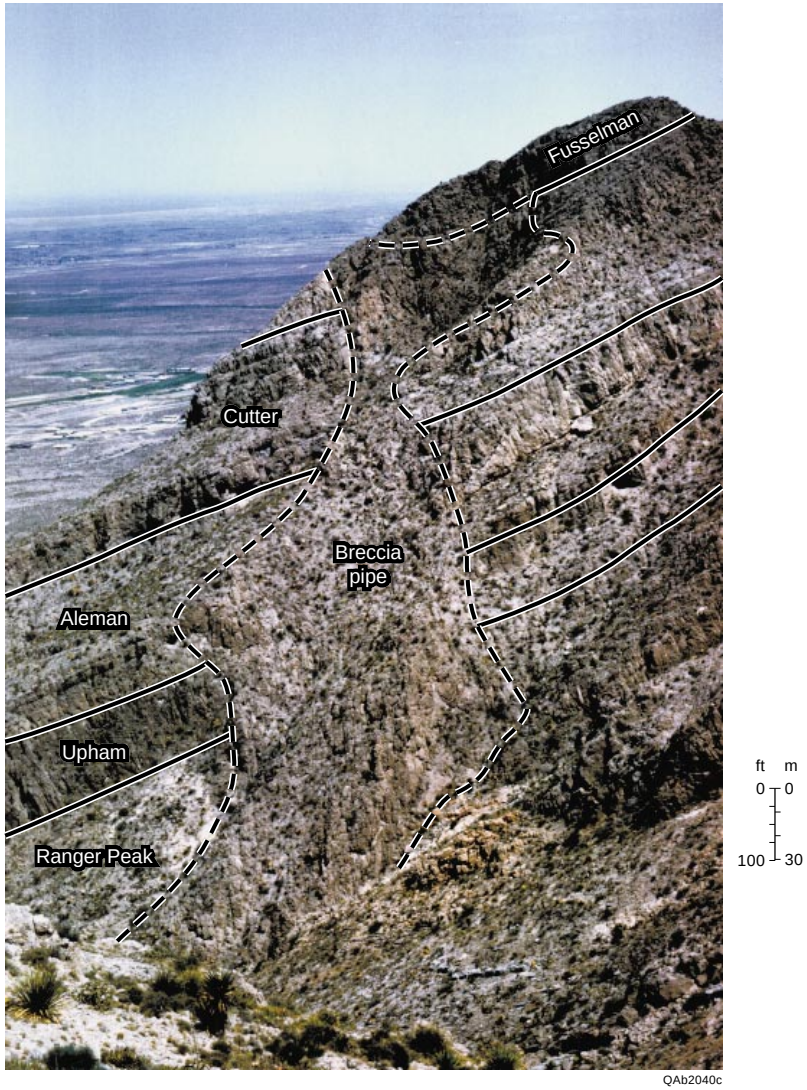

Figure 7. (d) Uninterpreted photograph of breccia pipe exposed in an unnamed Ellenburger outcrop in the Franklin Mountains (Courtesy F. J. Lucia, Bureau of Economic Geology). The Ranger Peak through Cutter section is Ordovician age (Ellenburger equivalent); the Fusselman is a Silurian unit. (e) Interpereted photograph of breccia pipe exposed in an unnamed Ellenburger outcrop in the Franklin Mountains (Courtesy F. J. Lucia, Bureau of Economic Geology). The Ranger Peak through Cutter section is Ordovician age (Ellenburger equivalent); the Fusselman is a Silurian unit.

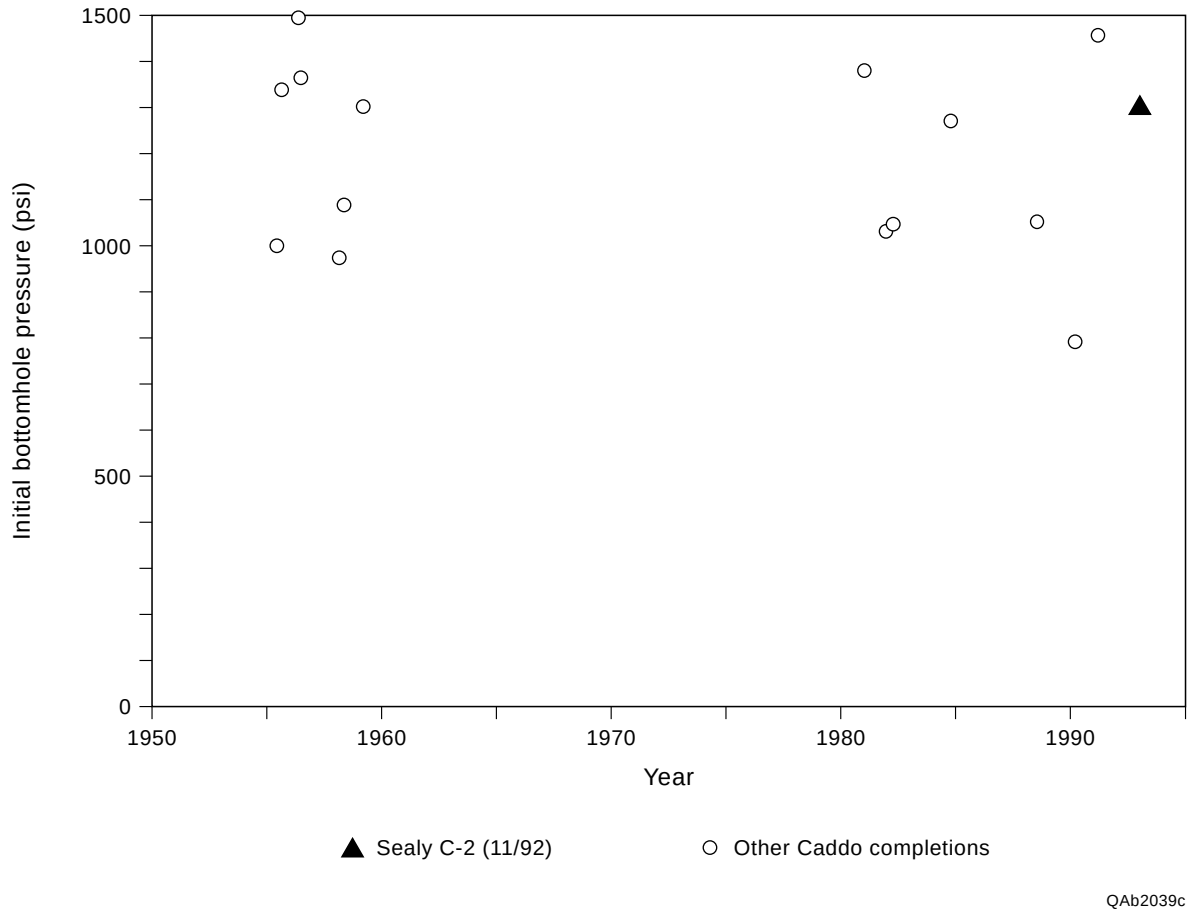

Figure8. Initial pressure measured in Sealy C-2 Caddo completion is comparable to initial pressures reported in other wells drilled in the Caddo sequence, implying little drainage associated with surrounding production.

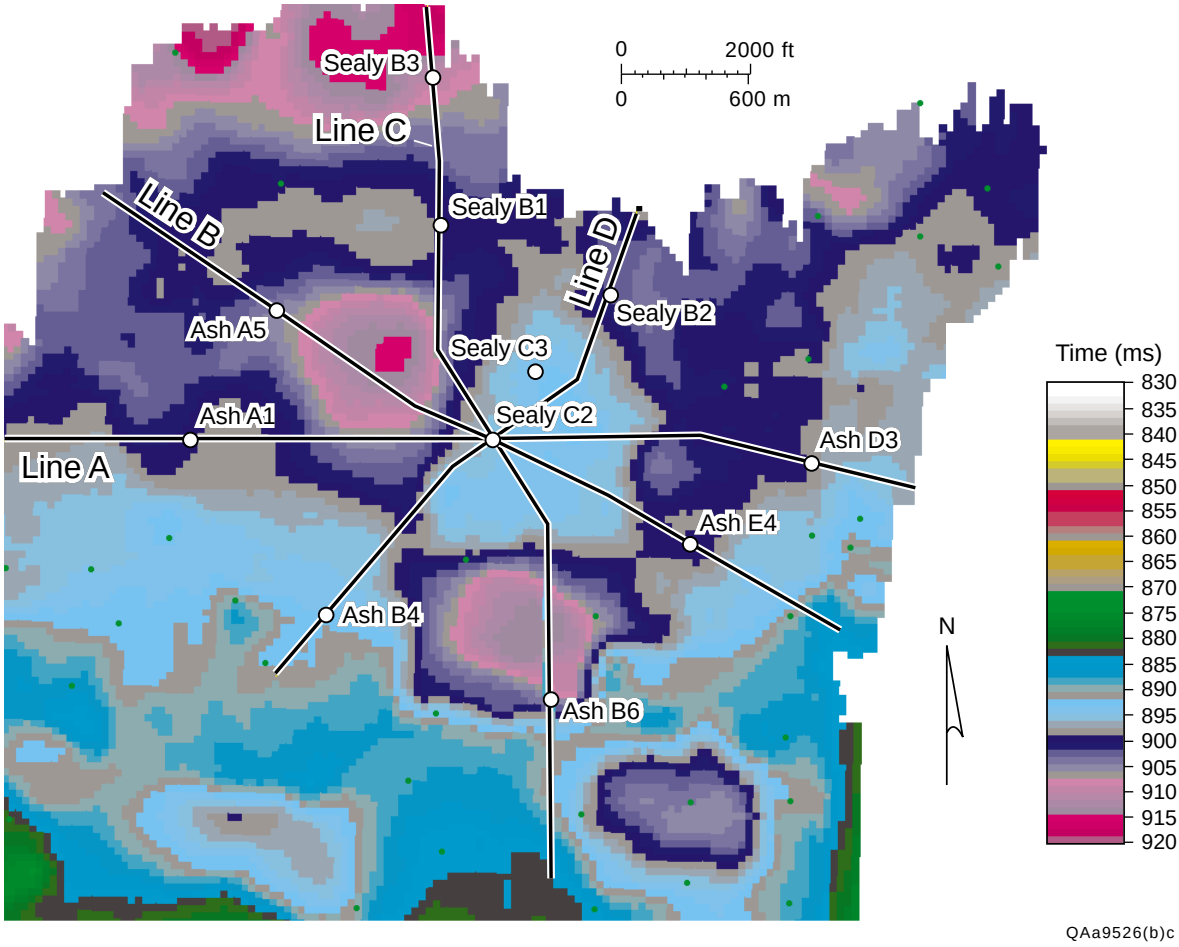

Figure 9. Time structure map of the Caddo in the vicinity of the Sealy C-2 well. The well is positioned on a structural high that was created when the surrounding strata sank into a ring of karst collapsed zones. The structural closure is approximately 130 acres. Our interpretation is that deep Ellenburger solution weathering produced karst collapses that extended vertically to disrupt this younger, Atokan surface, affect Pennsylvanian sedimentation, and compartmentalize several Bend Comglomerate reservoirs by subtle faults and structural sags.

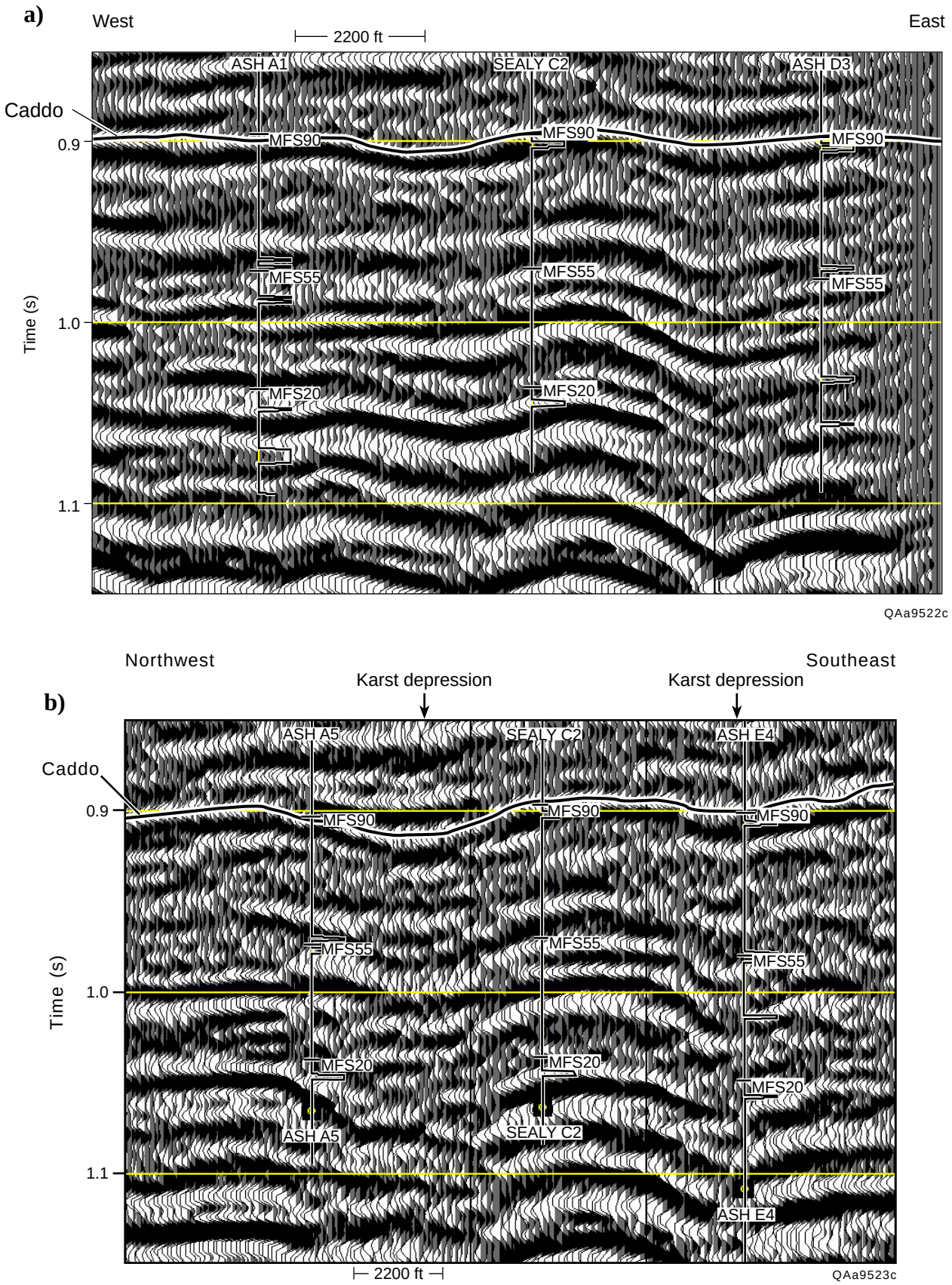

Figure 10. (a) Profile along Line A of Figure 9 showing how the Sealy C-2 Caddo reservoir is structurally compartmentalized by surrounding Ellenburger-related karst collapse zones. MFS90 is the position of the log-measured depth of the sequence boundary (maximum flooding surface) for the top of the Caddo, when that log depth is converted to seismic two-way traveltime. MFS55 is the log-measured top of the Bridgeport; MFS20 is the top of the Vineyard. The spikes on the curve plotted below each well name show where zones were perforated. (b) Profile along Line B showing how the Sealy C-2 Caddo reservoir is structurally compartmentalized by Ellenburger-related karst collapsed zones. (c) Profile along Line C, (d) Profile along Line D.

c)

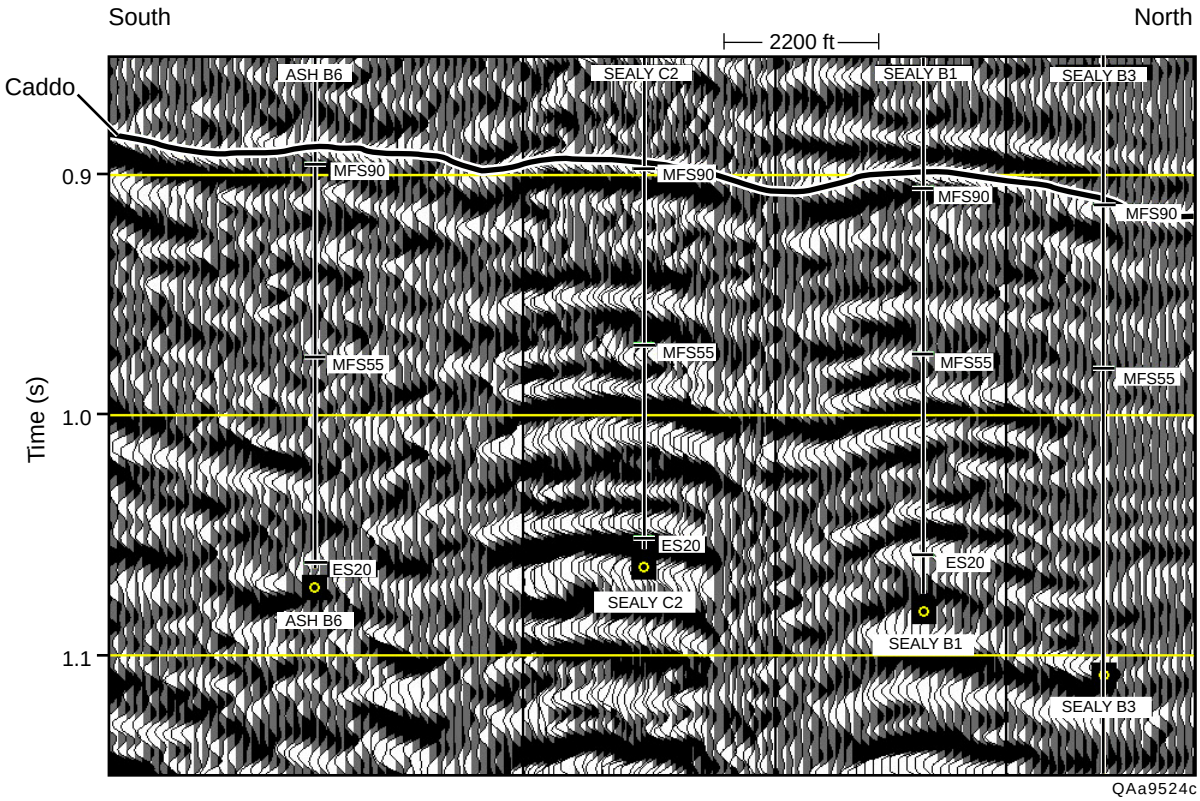

Figure 10. (c) Continued.

d)

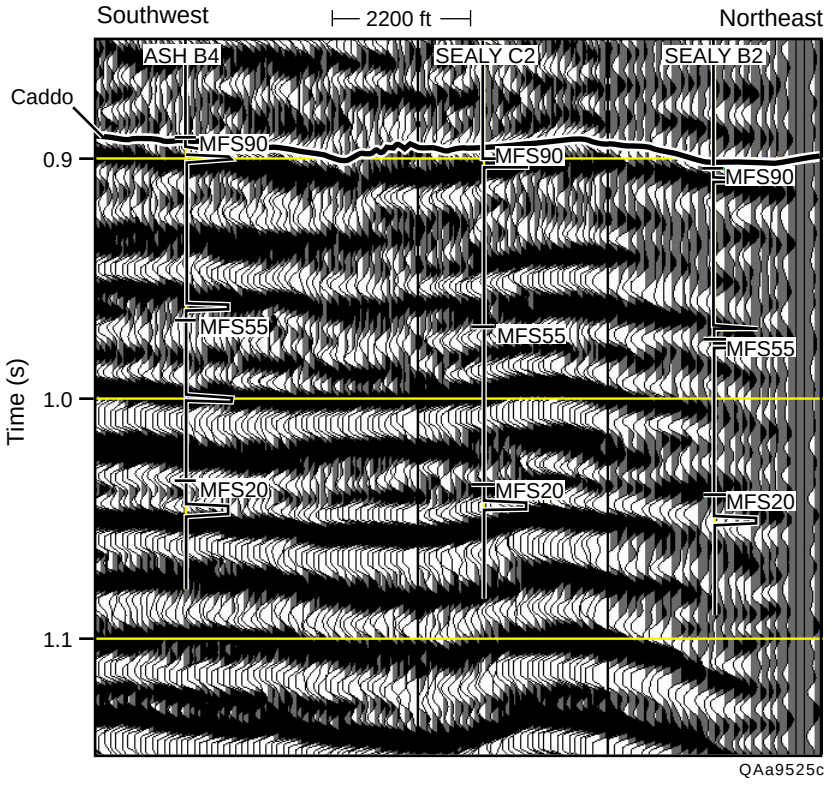

Figure 10. (d) Continued.

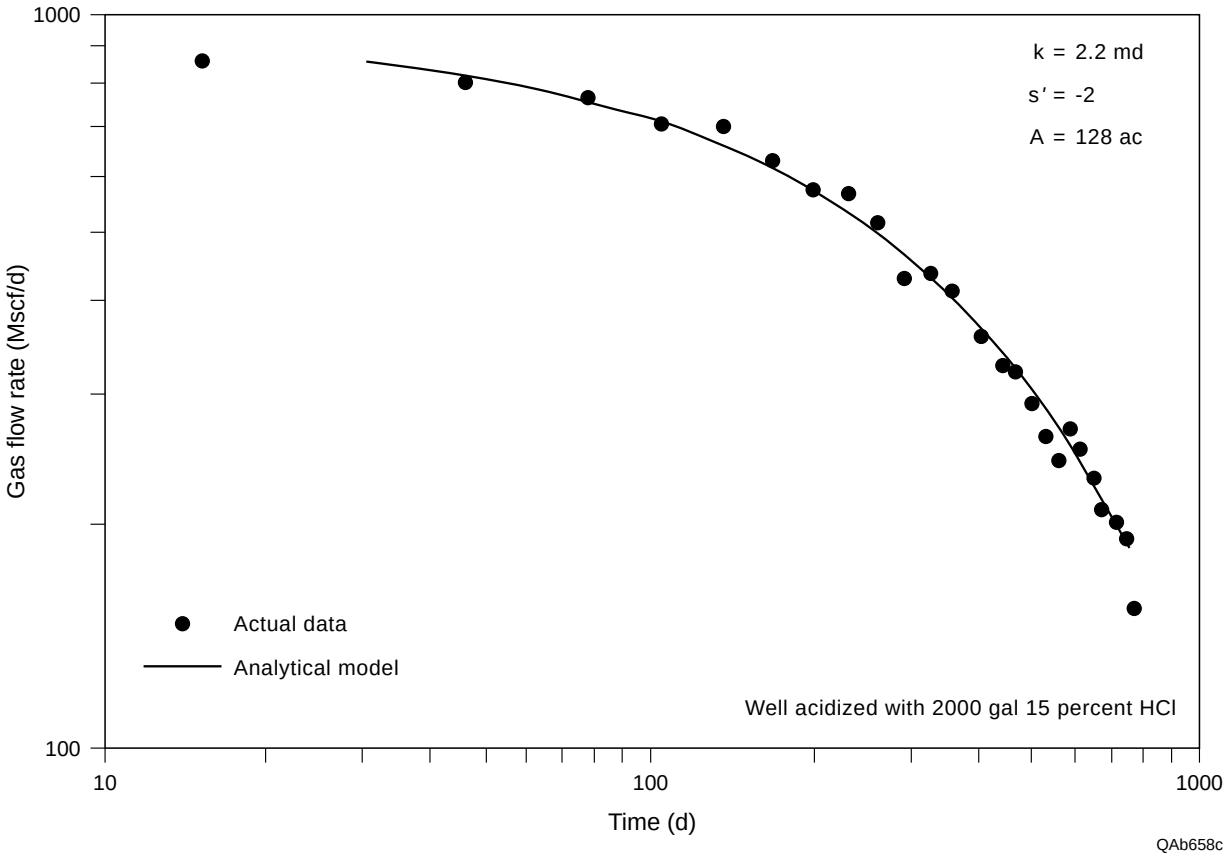

Figure 11. History match of production data from the Sealy C-2 well provides estimates of reservoir properties such as permeability and drainage area. The modeled areal size of the reservoir is 128 acres, essentially the same as the structural closure shown in Figure 9.